

1 **Modelled subglacial floods and tunnel valleys control the lifecycle of transitory ice**
2 **streams**

3 T. Lelandais^(a*), É. Ravier^(a), S. Pochat^(b), O. Bourgeois^(b), C.D. Clark^(c), R. Mourgues^(a) and P.
4 Strzeczynski^(a)

5 ^(a) Laboratoire de Planétologie et Géodynamique, UMR 6112, CNRS, Le Mans Université,
6 Avenue Olivier Messiaen, 72085 Le Mans Cedex 9, France

7 ^(b) Laboratoire de Planétologie et Géodynamique, UMR 6112, CNRS, Université de Nantes, 2
8 rue de la Houssinière, BP 92208, 44322 Nantes Cedex 3, France

9 ^(c) Department of Geography, University of Sheffield, Sheffield, UK

10 ^(*) Correspondence to: thomas.lelandais@univ-lemans.fr

11 **Ice streams are corridors of fast-flowing ice that control mass transfers from continental**
12 **ice sheets to oceans. Their flow speeds are known to accelerate and decelerate, their**
13 **activity to switch on and off, and even their locations to shift entirely. Our analogue**
14 **physical experiments reveal that a lifecycle incorporating evolving subglacial meltwater**
15 **routing and bed erosion can govern this complex transitory behaviour. The modelled ice**
16 **streams switch on and accelerate when subglacial water pockets drain as marginal**
17 **outburst floods (basal decoupling). Then they decelerate when the lubricating water**
18 **drainage system spontaneously organising itself into channels that create tunnel valleys**
19 **(partial basal recoupling). The ice streams surge or jump in location when these water**
20 **drainage systems maintain low discharge but they ultimately switch off when tunnel**
21 **valleys have expanded to develop efficient drainage systems. Beyond reconciling**
22 **previously disconnected observations of modern and ancient ice streams into a single**
23 **lifecycle, the modelling suggests that tunnel valley development may be crucial in**
24 **stabilising portions of ice sheets during periods of climate change.**

25 **Keywords:** ice streams, experimental modelling, subglacial meltwater drainage, tunnel
26 valleys, subglacial outburst floods

27 1. Introduction

28 Continental ice sheets currently store the equivalent of a 65 m thick global equivalent
29 water layer and have been major contributors to the nearly 85 mm global sea level rise measured
30 between 1993 and 2017 (Vaughan et al., 2013; Beckley et al., 2015). The mass transfer from
31 these ice sheets to the ocean is spatially heterogeneous: approximately 80% of the ice discharge
32 is focused in a finite number of ice streams, which act as preferential drainage pathways for
33 meltwater also (Bamber et al., 2000; Bennett, 2003).

34 Modern and ancient ice streams are typically hundreds of kilometres long and a few
35 kilometres to tens of kilometres wide, with ice velocities of the order 10^2 to 10^4 m/yr. Despite
36 the fact that they occurred and occur in all former and modern ice sheets, their initiation, and
37 the controls on their dynamics and evolution remain debated. Numerical modelling suggests
38 that ice flow might self-organise into regularly-spaced ice streams as a consequence of
39 thermomechanical feedbacks within ice (Payne and Dongelmans, 1997; Hindmarsh, 2009) or

40 because of inherent instability of thin subglacial meltwater films (Kyrke-Smith et al., 2014).
41 Numerous observations however, have highlighted preferential location of ice streams at sites
42 of specific bed properties such as in topographic troughs, over areas of soft sedimentary
43 geology, zones of higher geothermal heat flux or as a consequence of where subglacial
44 meltwater is routed (Winsborrow et al., 2010; Kleiner and Humbert, 2014). These viewpoints
45 might not be mutually exclusive if self-organisation into regularly-spaced streams is the
46 primary control but that it is strongly mediated by local bed templates (e.g. troughs) or events
47 (meltwater drainage) that initiate or anchor streams in certain locations. Exploring this
48 hypothesis by numerical modelling has not yet been achieved because of uncertainties in how
49 to formulate basal ice flow in relation to bed friction, and due to challenges of including all
50 potentially relevant processes, especially so for subglacial water flow (Flowers, 2015).

51 Observations of spatial and temporal variations in the activity of ice streams against
52 fluctuations in their subglacial hydrology indicate that the style and flux of water drainage is a
53 major component driving change. Examples include: reorganisation of subglacial drainage
54 systems (Elsworth and Suckale, 2016), subglacial water piracy (Vaughan et al., 2008; Carter et
55 al., 2013), and development and migration of transient subglacial water pockets (Gray et al.,
56 2005; Peters et al., 2007; Siegfried et al., 2016). However, these variations have been observed
57 or inferred independently, at different places and on yearly timescales, thus limiting our
58 understanding of the true role of the subglacial hydrology as primary or secondary drivers of
59 ice stream changes. In this paper, we circumvent the challenge of numerically modelling ice
60 stream initiation and dynamics, including subglacial water drainage, by exploiting a physical
61 laboratory approach that simultaneously combines silicon flow, water drainage and bed erosion.

62 Connections between ice stream activity and subglacial hydrology are supported by the
63 occurrence of geomorphic markers of meltwater drainage on ancient ice stream beds (e.g.
64 meltwater channels, tunnel valleys, eskers) (Patterson, 1997; Margold et al., 2015; Livingstone
65 et al., 2016). Among these markers, tunnel valleys deserve specific attention because they have
66 high discharge capacities and, as such, may be major contributors to the release of meltwater
67 and sediment to the ocean and may promote ice sheet stability by reducing the lubricating effect
68 of high basal water pressure. These valleys are elongated and over-deepened hollows, ranging
69 from a few kilometres to hundreds of kilometres long, from hundreds metres to several
70 kilometres wide and from metres to hundreds of metres deep. Their initiation is generally
71 attributed to subglacial meltwater erosion but their development processes (in time and space)
72 and their relationship to ice streaming are still debated. Indeed, ice streams commonly operate
73 because of high basal water pressure while the development of a tunnel valleys system generally
74 leads to enhanced drainage efficiency and basal water pressure reduction (Engelhardt et al.,
75 1990; Marciznek and Piotrowski, 2006; Kyrke-Smith et al., 2014).

76 Several field studies have already suggested a connection between catastrophic glacial
77 outburst floods at ice sheets margins and a suite of events involving ice streaming, tunnel valley
78 development and stagnation of the ice margin. (Jørgensen and Piotrowski, 2003; Alley et al.,
79 2006; Hooke and Jennings, 2006; Bell et al., 2007). Such outburst floods can profoundly and
80 rapidly alter the oceanic environment by transferring considerable amounts of ice, freshwater,

81 and sediment from continents to oceans (Evatt et al., 2006). The suspected connection between
82 ice streams, tunnel valleys, and outburst floods have never been observed or modelled however.

83 Here, we describe the results of a physical experiment performed with an innovative
84 analogue modelling device that provides simultaneous constraints on ice flow, subglacial
85 meltwater drainage, subglacial sediment transport and subglacial landform development
86 (Lelandais et al., 2016; Fig. 1). We propose that the location and initiation of ice streams might
87 arise from subglacial meltwater pocket migration and drainage pathways and that the evolution
88 of ice stream dynamics is subsequently controlled by subglacial drainage reorganization and
89 tunnel valley development. This study reconciles into a single story several detached inferences,
90 derived from observations at different timescales and at different places on modern and ancient
91 ice streams.

92 2. Experimental ice stream model

93 Ice stream dynamics are controlled by various processes that act at different spatial and
94 temporal scales; they also involve several components with complex thermo-mechanical
95 behaviours (ice, water, till, bedrock) (Paterson, 1994). Considering all these processes and
96 components simultaneously, together with processes of subglacial erosion, is thus a challenge
97 for numerical computational modelling (Fowler and Johnson, 1995; Marshall, 2005; Bingham
98 et al., 2010). Some attempts in analogue modelling have been made to improve our knowledge
99 on subglacial erosional processes by meltwater (Catania and Paola, 2001) or gravity current
100 instabilities produced by lubrication (Kowal and Worster, 2015). To combine ice flow
101 dynamics and erosional aspects in a single model, we designed an alternative experimental
102 approach that allows simultaneous modelling of ice flow, subglacial hydrology and
103 sedimentary/geomorphic processes. With all the precautions inherent in using analogue
104 modelling, our experiments reproduce morphologies and dynamics that compare well with
105 subglacial landforms and ice stream dynamics despite some differences in spatial and temporal
106 scales and a number of active processes (e.g. Paola et al., 2009).

107 2.1. Experimental apparatus

108 The model is set in a glass box (70 cm long, 70 cm wide and 5 cm deep) (Fig. 1). A 5 cm thick,
109 flat, horizontal, permeable and erodible substratum, made of sand ($d_{50}=100\ \mu\text{m}$) saturated with
110 pure water and compacted to ensure homogeneous values for its density ($\rho_{\text{bulk}} = 2000\ \text{kg/m}^3$),
111 porosity ($\Phi = 41\ \%$) and permeability ($K = 10^{-4}\ \text{m/s}$), rests on the box floor. The ice sheet
112 portion is modelled with a 3 cm thick layer of viscous ($\eta = 5 \cdot 10^4\ \text{Pa s}$) and transparent but
113 refractive ($n = 1.47$) silicon putty placed on the substratum. The model is not designed to
114 simulate an entire ice sheet. The silicon layer is circular in plan view (radius = 15 cm) to avoid
115 lateral boundary effects on silicon flow. Subglacial meltwater production is simulated by
116 injection of water with a punctual injector, 4 mm in radius, placed at a depth of 1.8 cm in the
117 substratum and connected to a pump (Fig. 1). The injector is located below the centre of the
118 silicon layer to be consistent with the circular geometry of the experiment. The water discharge
119 is constant ($1.5\ \text{dm}^3/\text{h}$) over the duration of the experiment and generates water flow at the
120 silicon-substratum interface and within the substratum. Water discharge is calculated
121 beforehand so that water pressure exceeds the combined weight of the sand and silicon layers.

122 The injection of water starts when the silicon layer reaches the dimensions we fixed for every
123 experiment (15 cm radius and 3 cm thickness) and a perfect transparency. Once injected, water
124 flow is divided into a Darcy flow within the substratum and a flow at the silicon/substratum
125 interface. The water flowing at the silicon/substratum interface originates from a pipe forming
126 at the injector once water pressure exceeds the cumulative pressure of the silicon and sand
127 layers. The ratio between the Darcy flow and the flow at the silicon/substratum interface is
128 inferred from computations of the water discharge flowing through the pipe based on the
129 substratum properties and the input discharge. We estimate that 75% of the input discharge is
130 transferred as Darcy flow in the substratum and 25% of the input discharge along the
131 silicon/substratum interface.

132 2.2. Acquisition process and post-processing

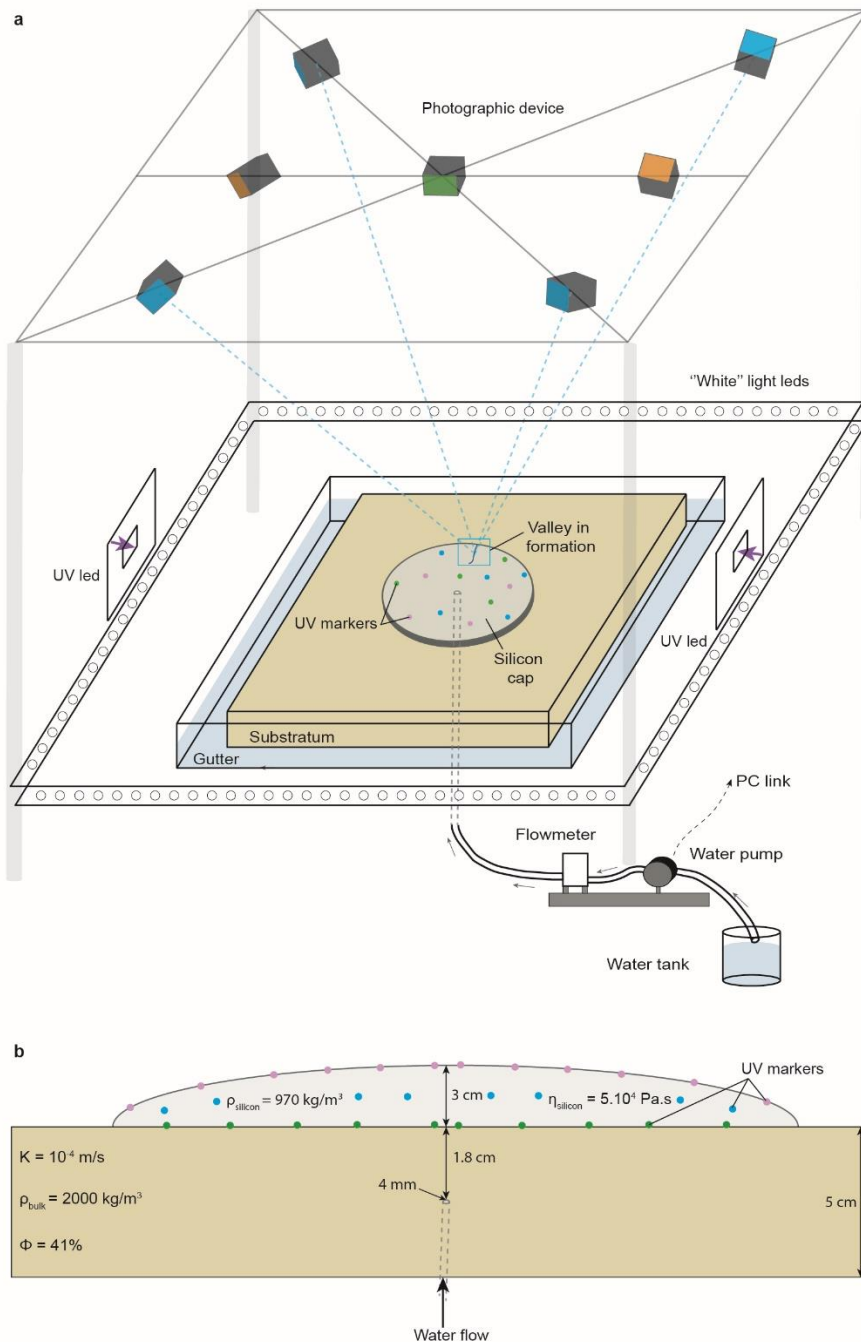
133 In order to monitor the development of landforms on the substratum, we use six
134 synchronised cameras equidistant from the experiment centre (Fig. 1) taking photographs of the
135 experiment every 5 seconds. Two cameras (orange on Fig. 1) cover the whole extent of the
136 experiment and four cameras (blue on Fig. 1) focus on specific regions to obtain higher
137 resolution images. These cameras take simultaneous pictures with differing positions and
138 orientations. Digital elevation models of the silicon surface and of the substratum are derived
139 from these images by photogrammetry. The ultimate stage of the experiment is to remove
140 distortions due to light refraction through the silicon putty and apply corrections to the
141 substratum topography. This treatment is achieved using a custom algorithm able to evaluate
142 the gap between the measured altitude and the real altitude of each pixel of the DEM (cf detailed
143 post-treatment methods in Lelandais et al., 2016). Tests performed on previously known
144 topographies show that the vertical precision of the retrieved digital elevation models is better
145 than 10^{-1} mm.

146 The flow velocity of the silicon layer is monitored near its base (V_{base}), at mid-depth (V_{mid}) and
147 at its surface (V_{surface}), with an additional camera placed over the centre of the experiment (green
148 on Fig. 1). For that purpose, the camera records the position on pictures taken at regular time
149 intervals in ultraviolet (UV) of 180 UV paint drops (1 mm in radius) placed at 1 mm above the
150 base, at mid-depth and at the surface of the silicon layer (Figs. 1, S1). The monitoring of every
151 UV marker position through time was used to produce velocity and vertical displacement maps.
152 Vertical displacement maps are interpolated from the subtraction of the DEM at time t with the
153 DEM generated from the photographs taken a few seconds before the injection. Velocity maps
154 are interpolated from the subtraction of the position of every marker at time t with the position
155 of the same markers at the previous stage. These passive markers are transparent at visible
156 wavelengths and do not alter pictures of the substratum taken through the silicon cap. They
157 represent less than 0.5% of the silicon layer in volume and tests have shown that they do not
158 affect its overall rheological behaviour. Uncertainties in the measured position of markers on
159 images are less than one pixel in size (i.e. less than 10^{-1} mm), thus uncertainties in the derived
160 velocities are comprised between $5 \cdot 10^{-4}$ and $2 \cdot 10^{-3}$ mm/s, depending on the time interval
161 between photographs.

162

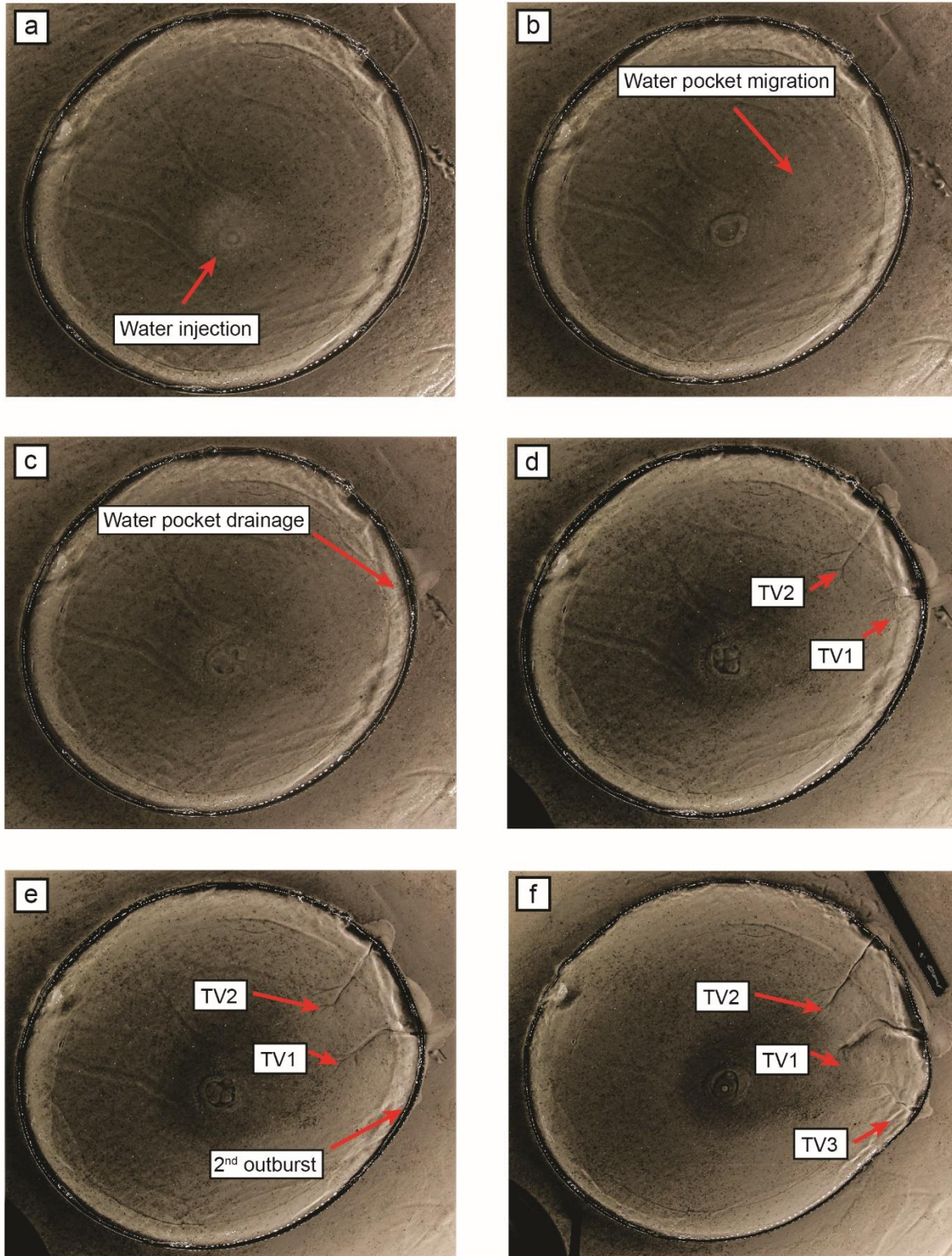
163 2.3. Scaling and limitations

164 In this study, we focus our attention on the relations between subglacial water flow,
165 subglacial erosion and ice flow using an experiment approach. Considering that in our model
166 meltwater is simulated by an injection of water, the rules of a classical scaling where the model
167 is a perfect miniaturisation of nature are not practical (Paola et al., 2009). In this perspective,
168 we base the scaling of our model on the displacement of the natural ice and experimental silicon
169 margins through time. We use a unit-free speed ratio between the silicon/ice margin velocity
170 and the incision rate of experimental/natural tunnel valleys. In this way, the complexity of the
171 relations between subglacial hydrology, subglacial erosion and ice flow, which is one of the
172 main issue in numerical modelling, is included in the velocity values. The scaling attest that the
173 value of the ratio between margin velocity and incision rate of tunnel valleys in the experiment
174 fall within the field validity defined by the range of natural settings (full details in Lelandais et
175 al., 2016). The main scaling limit regards the viscosity ratios between glacier ice, silicon putty
176 and water. The size of the experimental ice stream, being partly controlled by the high silicon
177 viscosity, may be underestimated compared to the size of modelled tunnel valleys.
178 Considering that our model is a simplification of nature, we cannot simulate the whole
179 complexity of the nature processes. In contrast with ice, the commercial silicon putty we use
180 (Dow Corning, SGM36) is impermeable, newtonian, isotropic, and its viscosity is nearly
181 independent of temperatures between 10 and 30°C. Therefore, rheological softening with strain
182 rate, temperature, anisotropy, and meltwater content (e.g. Bingham et al., 2010) cannot be
183 reproduced. The silicon putty cannot reproduce the ice/water phase transition either, requiring
184 the use of punctual water injection in the experiment. This punctual injection does not simulate
185 the mosaic of meltwater production regions existing beneath glaciers or the episodic input from
186 supraglacial/englacial meltwater reservoirs. Experimental meltwater routing is predominantly
187 controlled by the water discharge we inject in our system and therefore differs from parameters
188 controlling hydrology in glacial systems. Subglacial meltwater routing is indeed controlled by
189 the ice surface slope, the bed topography, and the glacier mass balance (Röthlisberger and Lang,
190 1987). The ice surface slope controls potentiometric surfaces, generally guiding subglacial
191 water flow parallel to ice sheet surfaces (Glen, 1954; Shreve, 1972; Fountain and Walder,
192 1998). Finally, the substratum we use is homogeneous, flat and composed of a well-sorted
193 mixture of sand-sized grains. This model, designed to decipher the interaction between
194 subglacial hydrology and ice dynamics, hinders the influence of bed topography and geology
195 (especially the influence of subglacial till) (Winsborrow et al., 2010). The deformation of the
196 subglacial till and its complex rheological behavior is known to promote ice streaming (Alley
197 et al., 1987), modify the subglacial hydrology, and alter the size of tunnel valleys. The
198 development of an analogue material scaled to reproduce subglacial till characteristics is
199 extremely difficult so we did not try to include the equivalent of a till layer in the experiment.
200 We thus assume that the velocity contrasts observed in the experiment are likely to be amplified
201 in natural ice sheets, by the complex rheological behaviour of ice and till. This may lead to the
202 development of narrower ice streams with higher relative velocities and sharper lateral shear
203 margins in natural ice sheets than in the experiment (Raymond, 1987; Perol et al., 2015).



204

205 **Figure 1.** Description of the analogue device used in this study. a, Overview of the analogue device.
 206 The analogue device consists in a 70 cm long, 70 cm wide and 5 cm deep glass box filled with saturated
 207 and compacted sand simulating the substratum. The ice sheet portion is simulated by a circular layer of
 208 silicon putty containing 3 levels of UV markers. Meltwater production is simulated by a central and
 209 punctual injection of pure water within the substratum. Five synchronized cameras placed above the
 210 silicon putty (in blue) focus on the tunnel valley system and are used to produce digital elevation models
 211 by photogrammetry. Another camera (in orange) takes overview photographs of the analogue device to
 212 follow the progress of the whole experiment. A last camera (in green) is positioned at the vertical of the
 213 silicon layer centre and is configured to take high-resolution photographs in black light of the UV
 214 markers (illuminated with two lateral UV led lights). b, Cross-sectional profile of the analogue device
 215 displaying the position of the UV markers and the physical characteristics of both the substratum and
 216 the silicon layer.



217

218 **Figure 2.** Temporal evolution of the experiment seen on raw photographs. a. Formation of a water
 219 pocket. b. Migration of the water pocket. c. Marginal drainage of the water pocket and onset of the
 220 silicon stream. d. Development of two tunnel valleys (TV1 and TV2). e. Drainage of a second water
 221 pocket and silicon stream migration. f. Development of a new generation of tunnel valleys (TV3) and
 222 silicon stream decay. Silicon flow velocity and silicon surface displacement maps corresponding to the
 223 six stages described here are presented in Figure 3.

224 3. Experimental results

225 3.1. Stage-by-stage experimental progress

226 This experiment was repeated 12 times with identical input parameters (a 30 mm-thick silicon
227 layer of 150 mm radius; constant water input of 1.5 dm³/h during 1800 s). After an initial
228 identical state, a six-stage ice stream lifecycle linking outburst flooding, transitory ice
229 streaming, and tunnel valley development has been observed for all these simulations (Figs. 2,
230 3).

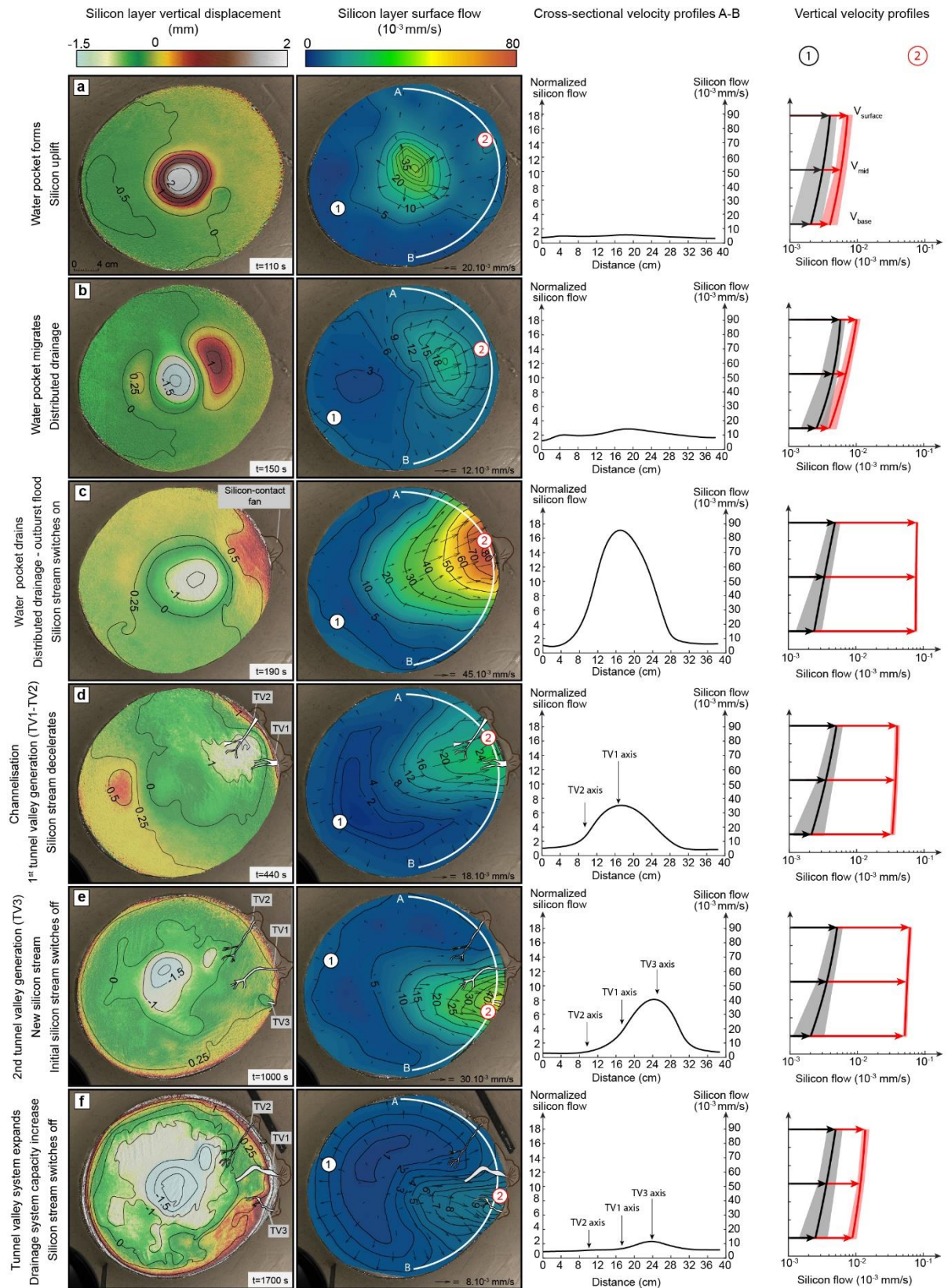
231 Initial state (Fig. S2). As long as no water is injected in the substratum, the silicon layer spreads
232 under its own weight and displays the typical parabolic surface profile of an ice sheet. It
233 increases in diameter and decreases in thickness with time, thus producing a radial pattern of
234 horizontal velocities, which increase in magnitude from the centre ($V_{\text{surface}} < 3 \cdot 10^{-3}$ mm/s) to the
235 margin ($V_{\text{surface}} = 8 \cdot 10^{-3}$ mm/s) (Fig. S2). V_{base} is close to 0 over the full extent of the silicon
236 layer ($\frac{V_{\text{base}}}{V_{\text{surface}}} \sim 0\%$), indicating coupling with the substratum. The silicon flow pattern changes
237 when meltwater production is simulated by injecting water at a constant discharge (1.5 dm³/h),
238 beneath the silicon layer.

239 Stage 1 (Figs. 2a, 3a). A water pocket grows below the centre of the silicon layer and raises its
240 surface by 2 mm. Above the water pocket, the silicon accelerates ($V_{\text{surface}} \geq 35 \cdot 10^{-3}$ mm/s), and
241 is decoupled from the substratum ($\frac{V_{\text{base}}}{V_{\text{surface}}} = 75$ to 80%). Below the rest of the silicon layer,
242 lower velocities ($V_{\text{surface}} = 8 \cdot 10^{-3}$ mm/s, $\frac{V_{\text{base}}}{V_{\text{surface}}} = 40$ to 50%) indicate higher basal friction.
243 These results are consistent with inferences that meltwater ponding can form pressurised
244 subglacial water pockets associated with basal decoupling, surface uplift, and ice flow
245 acceleration in natural ice sheets (e.g. Hanson et al., 1998; Elsworth and Suckale, 2016;
246 Livingstone et al., 2016). In the experiment however, these effects are restricted to an
247 approximately circular region and are not sufficient to produce channelised ice streaming.

248 Stage 2 (Figs. 2b, 3b). The water pocket expands and migrates towards the margin of the silicon
249 layer. The lack of channels incised in the substratum indicates that this displacement occurs as
250 distributed water drainage without any basal erosion. In the silicon layer, the region of surface
251 uplift, basal decoupling and acceleration ($V_{\text{surface}} = 18 \cdot 10^{-3}$ mm/s, $\frac{V_{\text{base}}}{V_{\text{surface}}} = 75$ to 85%)
252 expands and migrates downstream with the water pocket. Similar migrations of pressurised
253 subglacial water pockets have been observed or inferred under modern and ancient ice sheets
254 (Fricker et al., 2007; Carter et al., 2017), sometimes associated with migrations of regions of
255 ice surface uplift and ice flow acceleration (Bell et al., 2007; Stearns et al., 2008; Siegfried et
256 al., 2016). The experiment indicates that the migration of water pockets at the ice-bed interface
257 can contribute to the emergence of ice streams.

258

259



260

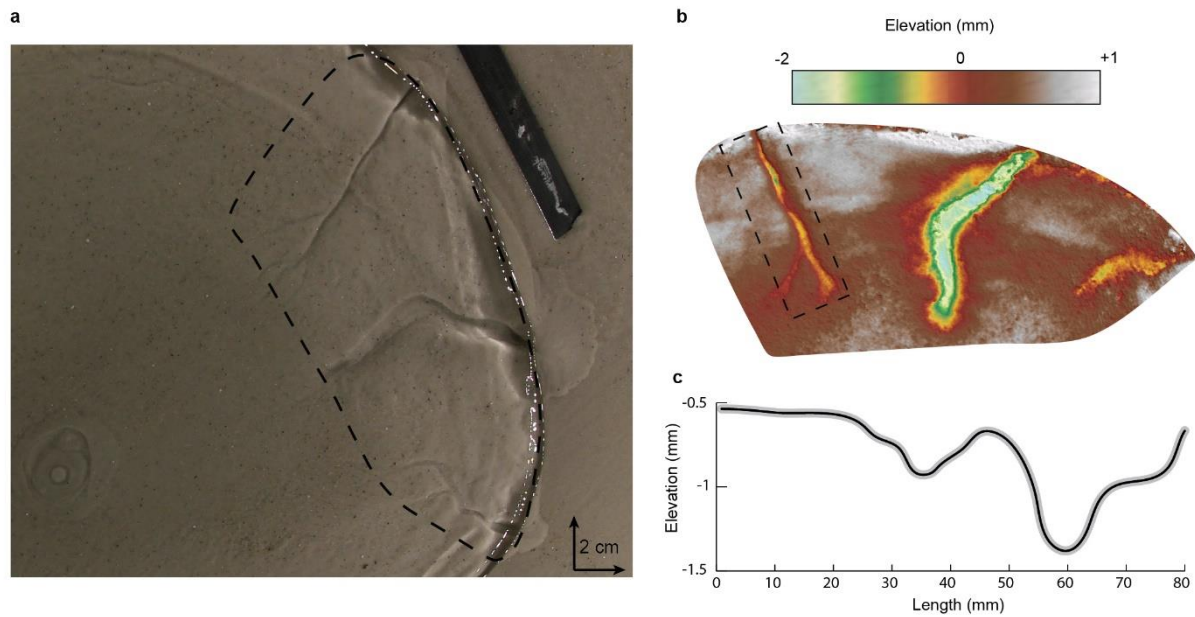
261 **Figure 3.** Temporal evolution of the experiment. a, Formation of water pocket, uplift of silicon surface
 262 uplift and acceleration. b, Migration of water pocket and overlying region of uplift and accelerated flow.
 263 c, Marginal drainage of water pocket and onset of silicon streaming. d, Tunnel valley development and
 264 silicon stream deceleration. e, Formation, migration and marginal drainage of a new water pocket,

265 development of a second silicon stream and of a new tunnel valley. f, Decay of the second silicon stream.
266 From left to right: (i) maps of vertical displacements of silicon layer surface, (ii) maps of horizontal
267 velocity at silicon layer surface, (iii) cross-sectional velocity profiles (absolute velocity on right axis,
268 velocity normalised by background velocity on left axis, profile locations indicated by white lines A-B
269 on maps), (iv) vertical velocity profiles for silicon stream (red profiles, locations labelled 2 on maps)
270 and for region opposed to silicon stream (black profiles, locations labelled 1 on maps).

271 Stage 3 (Figs. 2c, 3c). When the water pocket reaches the margin of the silicon layer, it drains
272 suddenly as a sheet flow. This marginal outburst flood is still fed by distributed drainage and
273 conveys sand particles eroded from the substratum towards a low-angle marginal sedimentary
274 fan (up to 40 mm long, 30 mm wide and 0.3 mm thick; Fig. S3). Simultaneously, the silicon
275 flow focuses in a stream (200 mm wide at the margin) that propagates upstream from the silicon
276 margin to the water injection area. This stream immediately peaks in velocity ($V_{\text{surface}} = 80 \cdot 10^{-3}$
277 mm/s , 16 times higher than the surrounding silicon) and is entirely decoupled from its
278 substratum ($\frac{V_{\text{base}}}{V_{\text{surface}}} > 90\%$). Although similar relations between outburst floods and ice flow
279 accelerations have been suspected in modern (Alley et al., 2006; Bell et al., 2007; Stearns et al.,
280 2008) and former (Livingstone et al., 2016) ice sheets, they have been documented for valley
281 glaciers only (e.g. Anderson et al., 2005). In these regions, they can produce sudden meltwater
282 discharges that exceed the capacity of distributed subglacial meltwater drainages and promote
283 basal decoupling and ice flow acceleration (e.g. Magnússon et al., 2007). The experiment
284 confirms that outburst floods can promote basal decoupling and trigger ice streaming in ice
285 sheets (Fowler and Johnson, 1995).

286 Stage 4 (Figs. 2d, 3d). The distributed subglacial drainage system starts to channelise: two
287 valleys (TV1 and TV2) appear below the margin of the silicon layer and gradually expand by
288 regressive erosion of the substratum. At this stage, TV1 is 30 mm long, 12 mm wide and 0.5
289 mm deep; TV2 is 80 mm long, 10 mm wide and 0.5 mm deep. These valleys, with their constant
290 widths, undulating long profiles and radial distribution, are analogue to natural tunnel valleys
291 in their dimensions, shapes, and spatial organization (Lelandais et al., 2016; Fig. 4). They are
292 fed by distributed water drainage. The sand eroded from the substratum transits through these
293 valleys and accumulates in high-angle marginal sedimentary fans, higher in elevation than the
294 valley floors (TV1 fan is up to 27 mm long, 30 mm wide and 0.5 mm thick; TV2 fan is up to
295 20 mm long, 24 mm wide and 1 mm thick; Fig. S3). In response to progressive channelisation
296 of the water drainage into the expanding valleys, the silicon stream narrows and slows down
297 (120 mm wide at the margin; $V_{\text{surface}} = 24 \cdot 10^{-3} \text{ mm/s}$). The silicon stream, still channelised, is
298 still flowing 8 times faster than the rest of the silicon layer and is still decoupled from the
299 substratum ($\frac{V_{\text{base}}}{V_{\text{surface}}} > 85\%$). These results are consistent with inferences that channelisation of
300 hitherto distributed subglacial water drainage systems can occur and reduce ice flow velocity
301 after outburst floods (Kamb, 1987; Retzlaff and Bentley, 1993; Magnússon et al., 2007), and
302 can be responsible for narrowing and deceleration of ice streams (Raymond, 1987; Retzlaff and
303 Bentley, 1993; Catania et al., 2006; Beem et al., 2014; Kim et al., 2016). At this stage of the
304 experiment, this transition, which corresponds to the initiation of tunnel valleys, is not sufficient
305 to stop ice streaming however.

306



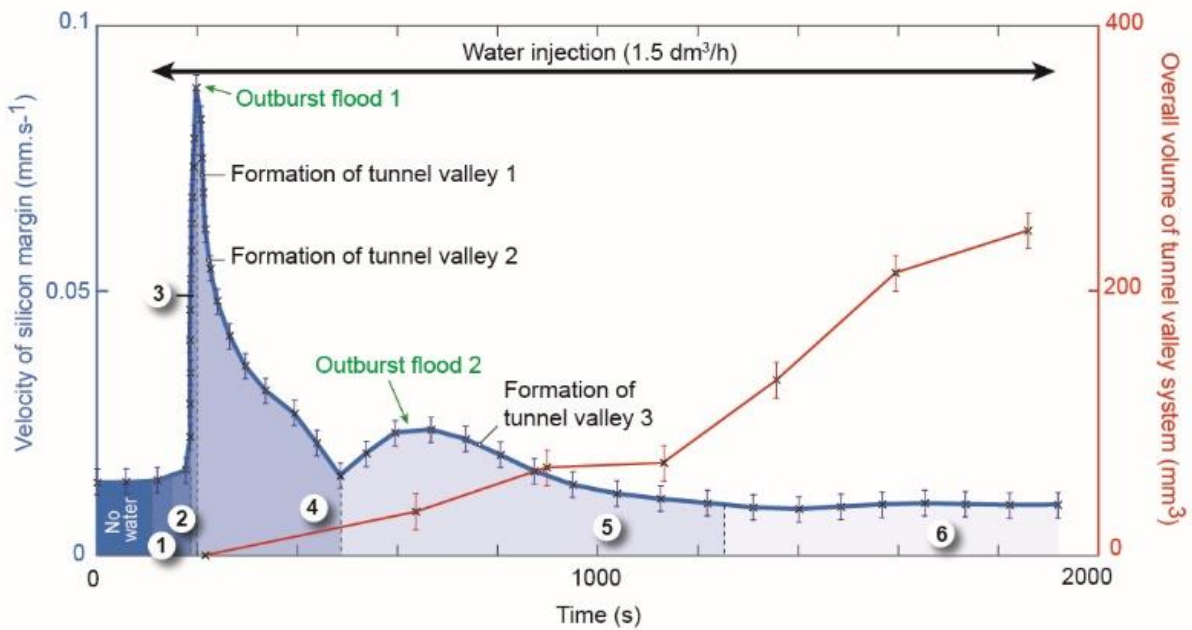
307

308 **Figure 4.** Digital Elevation Model (DEM) of an experimental tunnel valley and its associated
 309 longitudinal profile. a, Snapshot of the tunnel valley system. b, DEM of the tunnel valley corresponding
 310 to the one highlighted by a dashed box in a. c, Undulating longitudinal profile of the tunnel valley bottom
 311 extracted from the DEM in the dashed box shown in b.

312 Stage 5 (Figs. 2e, 3e). A new transient water pocket grows below the silicon layer, migrates and
 313 drains as an outburst flood, thus forming a new low-angle marginal sedimentary fan with at
 314 lateral offset of 4 cm with respect to TV1. This induces the activation of a second stream (V_{surface}
 315 $= 40 \cdot 10^{-3}$ mm/s) decoupled from its substratum ($\frac{V_{\text{base}}}{V_{\text{surface}}} = 80\%$) and the initiation of a new
 316 radial valley (TV3), in a hitherto slow-moving region of the silicon cap. Simultaneously, the
 317 first silicon stream switches off ($V_{\text{surface}} = 10 \cdot 10^{-3}$ mm/s), and recouple to its substratum
 318 ($\frac{V_{\text{base}}}{V_{\text{surface}}} = 30\%$), but water and sand still flow through TV1 and TV2. At this stage, TV1 is
 319 100 mm long, 8 mm wide and 0.7 mm deep and its fan is up to 21 mm long, 40 mm wide, and
 320 1.1 mm thick; TV2 is 80 mm long, 7.5 mm wide, and 0.6 mm deep and its fan is up to 20 mm
 321 long, 28 mm wide, and 1.6 mm thick. This result is consistent with inferences that natural ice
 322 streams can switch on and off, surge, and jump in location in response to changes in subglacial
 323 water drainage reorganisation (Catania et al., 2012; Le Brocq et al., 2013; Beem et al., 2014;
 324 Hulbe et al., 2016). The experiment further indicates that this complex behaviour is controlled
 325 by the growth and migration, in various possible directions, of transient pressurised subglacial
 326 water pockets that form successively as long as the discharge capacity of tunnel valleys systems
 327 is not sufficient to drain efficiently the available meltwater.

328 Stage 6 (Figs. 2f, 3f). Since their initiation, TV1, TV2, and TV3 have progressively increased
 329 in width, depth and length. At this stage TV1 is 100 mm long, 17 mm wide, and 1.2 mm deep
 330 and its fan is 28 mm long, 4 mm wide, and 1.5 mm high at the maximum; TV2 is 80 mm long,
 331 10 mm wide, and 0.8 mm deep and its fan is up to 16 mm long, 23 mm wide and 1.6 mm thick
 332 ; TV3 is 60 mm long, 11 mm wide, and 0.55 mm deep and its fan is up to 14 mm long, 23 mm
 333 wide, and 0.7 mm thick. Their overall volume and discharge capacity have thus increased (Fig.
 334 5). In response to this increased drainage efficiency, the second stream gradually decays (V_{surface}

335 $= 5 \cdot 10^3 \text{ mm} \cdot \text{s}^{-1}$), and recouples to its substratum ($\frac{V_{base}}{V_{surface}} = 35\%$). The silicon layer ultimately
 336 recovers a radial flow pattern (Fig. 3f). This result is consistent with the inference that ice
 337 streams may decelerate and even switch off in response to reduction of subglacial water
 338 pressures when efficient subglacial water drainage systems develop (Retzlaff and Bentley,
 339 1993; Beem et al., 2014; Livingstone et al., 2016; Kim et al., 2016). In the experiment, this
 340 development is governed by the expansion of tunnel valley networks. Large glaciotectonic
 341 thrust masses at the ice margin near tunnel valley fans are generally assumed to be field
 342 evidence of a fast ice flow stage prior to drainage through tunnel valleys (Hooke and Jennings,
 343 2006).



344
 345 **Figure 5.** Progressive expansion of overall volume of tunnel valleys system vs. velocity of silicon
 346 margin through the experiment. The circled numbers correspond to the six-stages of the proposed ice
 347 stream lifecycle.

348 3.2. Experimental reproducibility and variability

349 This experiment has been reproduced 12 times with identical input parameters. We always
 350 observe the same processes and events acting in a similar chronological order : (1) water pocket
 351 forms; (2) water pocket migrates; (3) water pocket drains (outburst flood) and silicon stream
 352 switches on; (4) Tunnel valleys form in response to channelisation; (5) silicon stream slows
 353 down and (6) finally switches off in response to the increase of drainage efficiency during
 354 tunnel valley development. However, despite this consistency in the progress of all simulations
 355 some variability has been detected. We measured different migration rates for the water pocket
 356 ranging from 30 s to 80 s that may result from small changes in subglacial topography and in
 357 the dynamics of silicon-bed decoupling. Considering a constant water discharge and the
 358 characteristics of the experiment, a longer period of migration implies: a longer period of water
 359 storage and a bigger water volume released at the silicon margin during the pocket drainage
 360 .We therefore recorded peak velocities for water pocket drainage ranging from $6 \cdot 10^{-3}$ to $12 \cdot 10^{-3}$
 361 mm/s . In response to variations of the water volume drained at the margin and peak discharge,

362 the maximum width of the silicon stream varies from 120 to 250 mm. The magnitude of the
363 outburst flood triggered during water pocket drainage also influences the amount of tunnel
364 valleys that subsequently form during the channelisation stage. A high magnitude outburst flood
365 generates a wider erosion beneath the silicon that will be suitable for the development of
366 multiple tunnel valleys. Hence, the amount of tunnel valleys at the end of the experiments
367 ranged from 1 to 5 with 1 to 3 tunnel valleys formed simultaneously during the initiation of the
368 channelisation stage. These valleys range from 40 to 120 mm long, 3 to 18 mm wide, and 0.3
369 to 1.8 mm deep. During tunnel valleys development, the evolution of drainage efficiency varies
370 between the experiments. A relatively inefficient system of tunnel valleys induces upstream
371 water pocket formation. As observed in Figure 3e, the drainage of this belated water pocket
372 may provoke water re-routing beneath the silicon layer and subsequent lateral migration of the
373 silicon stream. We counted 0 to 2 events of silicon stream migration for single experiments.
374 Finally, the time required to reach the phase of ice stream decay highly depends on the amount
375 of tunnel valleys formed during the experiments and their progressive development. We
376 observed a lifetime for the silicon stream ranging from 500 s to 1700 s, correlated with the
377 evolution of the drainage efficiency during tunnel valley development.

378 4. Proposed lifecycle of transitory ice streams

379 The experiment demonstrates that, on flat and homogenous beds, ice streams may arise,
380 progress, and decay in response to mechanical interactions between ice flow, subglacial water
381 drainage, and bed erosion. On uneven or heterogeneous beds (not simulated in this model),
382 these interactions may additionally be enhanced or disturbed by spatial variations in the
383 subglacial topography, geology, and geothermal heat flux (e.g. Bentley, 1987; Blankenship et
384 al., 1993; Anandakrishnan et al., 1998; Bourgeois et al., 2000; Winsborrow et al., 2010). The
385 complex rheology of glacial ice and subglacial till (both generally soften with increasing strain
386 rate, temperature, water content, and anisotropy) may also enhance these interactions by
387 increasing velocity contrasts between ice streams and their slower-moving margins. This may
388 lead to the development of narrower ice streams with higher velocities and sharper lateral shear
389 margins in natural ice sheets than in the experiment (Raymond, 1987; Perol et al., 2015).

390 Although the complexity of glacial systems cannot be fully modelled using the present
391 experimental setup, our results highlight the critical connection between ice streams and tunnel
392 valleys. As reviewed in Kehew et al., (2012) and suggested in Ravier et al., (2015) this relation
393 was suspected from the occurrence of tunnel valleys on ancient ice streams beds. However, it
394 raised a contradiction: subglacial meltwater pressures are generally supposed to be high below
395 ice streams (Bennett, 2003) while tunnel valleys are generally assumed to operate at lower water
396 pressures (Marczinek and Piotrowski, 2006). Although speculated from field evidences, our
397 results demonstrate that ice streaming, tunnel valley formation, release of marginal outburst
398 floods and subglacial water drainage reorganization may be interdependent parts of a single ice
399 stream lifecycle that involves temporal changes in subglacial meltwater pressures (Fig. 6).

400 1. Ice stream seeding. A prerequisite to the activation of ice streams is the formation of
401 pressurised subglacial pockets by meltwater ponding in ice sheet hinterlands. Approximately
402 circular regions of surface uplift and accelerated ice flow develop above these transient water
403 pockets.

404 2. Ice stream gestation. Pressurised water pockets migrate downstream by distributed water
405 flow. Regions of surface uplift and accelerated ice flow migrate accordingly.

406 3. Ice stream birth. Once water pockets reach ice sheet margins, they drain as outburst floods.
407 At that time, ice streams switch on, peak in velocity, and propagate towards ice sheet hinterlands
408 as decoupled corridors of accelerated ice flow underlain by pressurised distributed water
409 drainage.

410 4. Ice stream aging. Subglacial water drainage then channelises gradually: tunnel valleys fed
411 by pressurised distributed drainage start to form at ice stream fronts. Subsequent expansion of
412 tunnel valleys by regressive erosion progressively increases their overall discharge capacity,
413 lowers subglacial water pressures and provokes gradual ice stream recoupling and deceleration.
414 The response of ice stream dynamics to drainage channelisation and tunnel valley development
415 might be underestimated due to the high erodability of the subglacial bed used in the
416 experiment.

417 5. Ice stream rebirth (relocation or surge). As long as tunnel valley systems keep low drainage
418 capacities, successive pressurised subglacial water pockets can form, migrate, and drain as
419 marginal outburst floods. On even and homogeneous ice sheet beds, the subglacial water
420 drainage is controlled by the surface topography of ice sheets: subtle temporal changes in this
421 topography may thus be able to produce consecutive generations of ice streams and tunnel
422 valleys at different locations and with different flow directions. These jumps in locations and
423 directions may be responsible for the formation of independent, but sometimes intersecting, ice
424 streams corridors and tunnel valleys networks on some ancient ice sheet beds (Fowler and
425 Johnson, 1995; Jørgensen and Piotrowski, 2003). By contrast, if subglacial water routes and ice
426 flow are constrained by bed heterogeneities, migration of successive subglacial water pockets
427 along predetermined paths may induce sequential ice stream surges (Fowler and Johnson, 1995;
428 Hulbe et al., 2016) and participate in the gradual development of complex tunnel valley systems
429 at fixed places, like the Dry Valleys “Labyrinth” in Antarctica (Lewis et al., 2006).

430 6. Ice stream senescence. Ice streams may ultimately switch off when drainage capacities of
431 tunnel valley systems are sufficient to limit subglacial water overpressures. The progressive
432 decay of an ice stream activity can be partially produced by the thinning of the ice layer and the
433 subsequent reduction of the stress driving ice flow in ice stream corridors (Robel et al., 2013).
434 Our experiments display negligible thinning prior to ice stream decay. A constant water
435 discharge being applied in experiments, we demonstrate that increased drainage efficiency
436 during tunnel valley development can solely be responsible for ice stream slowdown. Tunnel
437 valleys and ice streams are frequently found to co-exist as exemplified by the many examples
438 reported from the southern margin of the Laurentide Ice Sheet (Patterson, 1997; Livingstone
439 and Clark, 2016). In one case, development of tunnel valleys has been suggested to have led to
440 stagnation of ice flow at an ice stream terminus (Patterson, 1997), a process that we have now
441 demonstrated by modelling. This further indicates that tunnel valleys development could secure
442 ice sheet stability as hinted by Marczynek and Piotrowski, (2006) by preventing ice stream
443 destabilisation. We apply a constant meltwater discharge to our model, however meltwater
444 production and discharge in a subglacial system fluctuates at different time scales (day, year,
445 decades). Fluctuating water production may have further implication on the size of ice streams,

446 the size and amount of tunnel valleys that develop through time, and the timescale involved in
447 ice sheet destabilization and stabilization. The oscillation in water production could strengthen
448 and multiply the life cycles of some transitory ice streams, already deciphered with a constant
449 water discharge in this study.

450 In a global change context, phenomena of ice stream stabilisation would requires that pre-
451 existing and newly forming tunnel valley systems expand sufficiently fast to accommodate
452 increased meltwater production. Investigating the processes and rates of tunnel valley
453 development are more than ever warranted to better assess ancient and present-day ice sheets
454 behaviour.

455

456

457

458

459

460

461

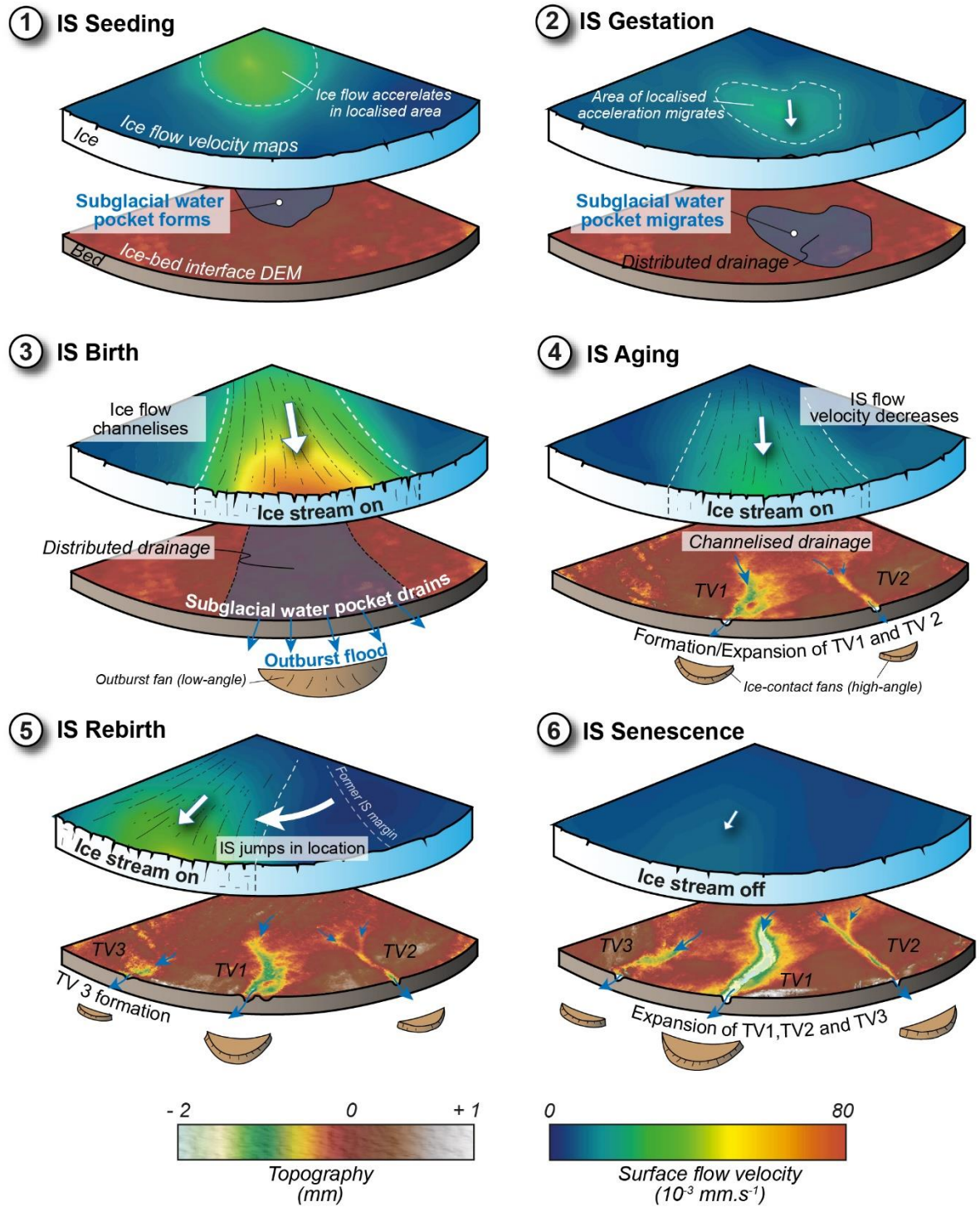
462

463

464

465

466



467

468 **Figure 6.** Chronological sequence with interpretative sketches illustrating the proposed ice
 469 stream lifecycle and the relations with tunnel valley development. Basal topography and surface
 470 flow velocity maps are derived from the experiment.

471

472

473

474 5. Conclusion

475 The transitory and mobile nature of ice streams may be understood in the framework of a
476 model lifecycle that involves temporal changes in subglacial meltwater pressures and arises
477 from interactions between ice flow, subglacial water drainage and bed erosion. In this model
478 lifecycle transitory ice streams arise, progress and decay in response to subglacial flooding,
479 changes in type and efficiency of subglacial drainage, and development of tunnel valleys. These
480 results are consistent with (and reconcile) a variety of otherwise detached observations
481 performed at different timescales and at different places, on modern and ancient natural ice
482 streams. One of the most novel outcomes of this study, is that subglacial tunnel valley
483 development may be crucial in controlling ice stream vanishing and perhaps, as a consequence,
484 in preventing catastrophic ice sheet collapses during periods of climate change. The processes
485 and rates of tunnel valley development are thus major issues for predicting the forthcoming
486 behaviour of present-day ice sheets and for assessing their contribution to the release of ice and
487 freshwater to the ocean. The innovative experimental approach, used here opens new
488 perspectives on the understanding of subglacial processes controlling ice sheet dynamics and
489 destabilisation.

490 **Author contributions:**

491 OB, RM, ER and SP conceived this research and gathered funding. TL designed and conducted
492 the experiments (setup, monitoring and post-treatment), with contributions by RM and PS. TL,
493 ER, OB, CDC, SP and RM contributed to the interpretation of the results and of their natural
494 implications. TL wrote the first draft of the manuscript; ER, OB, SP and CDC contributed
495 substantially to its present version.

496 **Competing interests:**

497 The authors declare that they have no conflict of interest

498 **Acknowledgements:**

499 This study is part of the DEFORm project (Deformation and Erosion by Fluid Overpressure)
500 funded by “Région Pays de la Loire”. Additional financial support was provided by the French
501 “Agence Nationale de la Recherche” through grant ANR-12-BS06-0014 ‘SEQSTRAT-ICE’
502 and the “Institut National des Sciences de l’Univers” (INSU) through the ‘Programme National
503 de Planétologie’ (PNP) and ‘Système Terre : Processus et Couplages’ (SYSTER) programs.

504 **References**

505 Alley, R. B., Blankenship, D. D., Rooney, S. T. and Bentley, C. R.: Till beneath ice stream B:
506 4. A coupled ice-till flow model, *J. Geophys. Res. Solid Earth.*, 92, 8931–8940, doi:
507 10.1029/JB092iB09p08931, 1987.

508
509 Alley, R. B., Dupont, T. K., Parizek, B. R., Anandkrishnan, S., Lawson, D. E., Larson, G. J.,
510 and Evenson, E. B.: Outburst flooding and the initiation of ice-stream surges in response to
511 climatic cooling: A hypothesis, *Geomorphology.*, 75, 76–89,
512 doi:10.1016/j.geomorph.2004.01.011, 2006.

513
514 Anandakrishnan, S., Blankenship, D. D., Alley, R. B., and Stoffa, P. L.: Influence of subglacial
515 geology on the position of a West Antarctic ice stream from seismic observations, *Nature.*,
516 394(6688), 62–65, doi: 10.1038/27889, 1998.

517
518 Anderson, R. S., Walder, J. S., Anderson, S. P., Trabant, D. C. and Fountain, A. G.: The
519 dynamic response of Kennicott Glacier , Alaska , USA , to the Hidden Creek Lake outburst
520 flood, *Annals of Glaciology.*, 40, 237–242, doi: 10.3189/172756405781813438, 2005.

521
522 Bamber, J. L., Vaughan, D. G. & Joughin, I.: Widespread Complex Flow in the Interior of the
523 Antarctic Ice Sheet, *Science.*, 287, 1248–1250, doi: 10.1126/science.287.5456.1248, 2000.

524
525 Beckley, B.; Zelensky, N.P.; Holmes, S.A.;Lemoine, F.G.; Ray, R.D.; Mitchum, G.T.; Desai,
526 S.; Brown, S.T.. 2015. Global Mean Sea Level Trend from Integrated Multi-Mission Ocean
527 Altimeters TOPEX/Poseidon Jason-1 and OSTM/Jason-2 Version 3. Ver. 3. PO.DAAC, CA,
528 USA. Dataset accessed at <http://dx.doi.org/10.5067/GMSLM-TJ123>.

529
530 Beem, L. H., Tulaczyk, S. M., King, M. A., Bougamont, M., Fricker, H. A., and Christoffersen,
531 P.: Variable deceleration of Whillans Ice Stream, West Antarctica, *J. Geophys. Res. Earth Surf.*,
532 119, 212–224, doi: 10.1002/2013JF002958, 2014.

533
534 Bell, R. E., Studinger, M., Shuman, C. A., Fahnestock, M. A. and Joughin, I.: Large subglacial
535 lakes in East Antarctica at the onset of fast-flowing ice streams, *Nature.*, 445, 904–907, doi:
536 10.1038/nature05554, 2007.

537
538 Bennett, M. R.: Ice streams as the arteries of an ice sheet: their mechanics, stability and
539 significance, *Earth-Science Rev.*, 61, 309–339, doi: 10.1016/S0012-8252(02)00130-7, 2003.

540
541 Bentley, C. R.: Antarctic ice streams: a review. *J. Geophys. Res. Solid Earth.*, 92(B9), 8843-
542 8858, doi: 10.1029/JB092iB09p08843, 1987.

543
544 Bingham, R. G., King, E. C., Smith, A. M. and Pritchard, H. D.: Glacial geomorphology:
545 towards a convergence of glaciology and geomorphology, *Prog. Phys. Geogr.*, 34, 327–355,
546 doi: 10.1177/0309133309360631, 2010.

547
548 Blankenship, D. D., Bell, R. E., Hodge, S. M., Brozena, J. M., Behrendt, J. C., and Finn, C. A.:
549 Active volcanism beneath the West Antarctic ice sheet and implications for ice-sheet stability,
550 *Nature.*, 361(6412), 526–529, doi: 10.1038/361526a0, 1993.

551
552 Bourgeois, O., Dauteuil, O., and Van Vliet-Lanoe, B.: Geothermal control on flow patterns in
553 the Last Glacial Maximum ice sheet of Iceland, *Earth Surf. Process and Landforms.*, 25, 59–
554 76, doi: 10.1002/(SICI)1096-9837(200001)25:1<59::AID-ESP48>3.0.CO;2-T, 2000.

555
556 Carter, S. P., Fricker, H. A., and Siegfried, M. R.: Evidence of rapid subglacial water piracy
557 under Whillans Ice Stream, West Antarctica, *Journal of Glaciology.*, 59, 1147–1162, doi:
10.3189/2013JoG13J085, 2013.

558

559 Carter, S. P., Fricker, H. A., and Siegfried, M. R.: Antarctic subglacial lakes drain through
560 sediment-floored canals: Theory and model testing on real and idealized domains, *Cryosph.*,
561 **11**, 381–405, doi: 10.5194/tc-11-381-2017, 2017.

562

563 Catania, G., and Paola, C.: Braiding under glass, *Geology.*, **29**, 259–262, doi: 10.1130/0091-
564 7613(2001)029<0259:BUG>2.0.CO;2, 2001.

565

566 Catania, G. A., Scambos, T. A., Conway, H., and Raymond, C. F.: Sequential stagnation of
567 Kamb ice stream, West Antarctica, *Geophys. Res. Lett.*, **33**(14), L14502 doi:
568 10.1029/2006GL026430, 2006.

569

570 Catania, G., Hulbe, C., Conway, H., Scambos, T. A., and Raymond, C. F.: Variability in the
571 mass flux of the Ross ice streams, West Antarctica, over the last millennium. *J. Glaciol.* **58**,
572 741–752, doi: 10.3189/2012JoG11J219, 2012.

573 Elsworth, C. W., and Suckale, J.: Rapid ice flow rearrangement induced by subglacial drainage
574 in West Antarctica, *Geophys. Res. Lett.*, **43**, 697–707, doi: 10.1002/2016GL070430, 2016.

575

576 Engelhardt, H., Humphrey, N., Kamb, B., and Fahnestock, M.: Physical conditions at the base
577 of a fast moving antarctic ice stream, *Science.*, **248**(4951), 57–59, doi:
578 10.1126/science.248.4951.57, 1990.

579

580 Evatt, G. W., Fowler, A. C., Clark, C. D., and Hulton, N. R. J.: Subglacial floods beneath ice
581 sheets, *Philos. Trans. R. Soc. London A Math. Phys. Eng. Sci.*, **364**, 1769–1794, doi:
582 10.1098/rsta.2006.1798, 2006.

583

584 Flowers, G. E.: Modelling water flow under glaciers and ice sheets, *Proc. R. Soc. A Math. Phys.*
585 *Eng. Sci.*, **471**(2176), 20140907, doi: 10.1098/rspa.2014.0907, 2015.

586

587 Fountain, A. G., and Walder, J. S.: Water flow through temperate glaciers, *Rev. Geophys.*, **36**,
588 299–328, doi: 10.1029/97RG03579, 1998.

589

590 Fowler, A. C., and Johnson, C.: Hydraulic run-away: a mechanism for thermally regulated
surges of ice sheets, *J. Glaciol.*, **41**, 454–461, doi: 10.3189/S002214300003478X, 1995.

591

592 Fricker, H. A., Scambos, T., Bindshadler, R., and Padman, L.: An active subglacial water
593 system in West Antarctica mapped from space, *Science.*, **315**, 1544–1548, doi:
10.1126/science.1136897, 2007.

594

595 Glen, J. W.: The stability of ice-dammed lakes and other water-filled holes in glaciers. *Journal*
of *Glaciology*, **2**(15), 316–318, doi: 10.3189/S0022143000025132, 1954.

596

597 Gray, L., Joughin, I., Tulaczyk, S., Spikes, V. B., Bindshadler, R., and Jezek, K.: Evidence for
598 subglacial water transport in the West Antarctic Ice Sheet through three-dimensional satellite
599 radar interferometry, *Geophys. Res. Lett.*, **32**, L03501, doi: 10.1029/2004GL021387, 2005.

600

601 Hanson, B., Hooke, R. L., and Grace, E. M.: Short-term velocity and water-pressure variations
602 down-glacier from a riegel, Storglaciären, Sweden. *Journal of Glaciology*, **44**(147), 359–367,
doi: 10.3189/S0022143000002689, 1998).

603 Hindmarsh, R. C. A.: Consistent generation of ice-streams via thermo-viscous instabilities
604 modulated by membrane stresses, *Geophys. Res. Lett.*, 36, L06502, doi:
605 10.1029/2008GL036877, 2009.
606

607 Hooke, R. L., and Jennings, C. E.: On the formation of the tunnel valleys of the southern
608 Laurentide ice sheet, *Quat. Sci. Rev.*, 25, 1364–1372, doi: 10.1016/j.quascirev.2006.01.018,
609 2006.
610

611 Hulbe, C.: Is ice sheet collapse in West Antarctica unstoppable?, *Science.*, 356, 910–911, doi:
612 10.1126/science.aam9728, 2017.
613

614 Hulbe, C. L., Scambos, T. A., Klinger, M., and Fahnestock, M. A.: Flow variability and ongoing
615 margin shifts on Bindschadler and MacAyeal Ice Streams, West Antarctica, *J. Geophys. Res.*
616 *Earth Surf.*, 121, 283–293, doi: 10.1002/2015JF003670, 2016.
617

618 Jørgensen, F., and Piotrowski, J. A.: Signature of the Baltic ice stream on Funen Island,
619 Denmark during the Weichselian glaciation, *Boreas.*, 32, 242–255, doi: 10.1111/j.1502-
620 3885.2003.tb01440.x, 2003.
621

622 Kamb, B.: Glacier surge mechanism based on linked cavity configuration of the basal water
623 conduit system, *J. Geophys. Res. Solid Earth.*, 92, 9083–9100, doi: 10.1029/JB092iB09p09083,
624 1987.
625

626 Kehew, A. E., Piotrowski, J. A., and Jørgensen, F.: Tunnel valleys: Concepts and controversies.
627 A review, *Earth-Science Rev.*, 113, 33–58, doi: 10.1016/j.earscirev.2012.02.002, 2012.
628

629 Kim, B.-H., Lee, C.-K., Seo, K.-W., Lee, W. S., and Scambos, T.: Active subglacial lakes
630 beneath the stagnant trunk of Kamb Ice Stream: evidence of channelized subglacial flow,
631 *Cryosph.*, 10, 2971-2980, <https://doi.org/10.5194/tc-10-2971-2016>, 2016.
632

633 Kleiner, T., and Humbert, A.: Numerical simulations of major ice streams in western
634 Dronning Maud Land, Antarctica, under wet and dry basal conditions, *J. Glaciol.*, 60, 215–
635 232, doi: 10.3189/2014JoG13J006, 2014.

636 Kowal, K. N., and Worster, M. G.: Lubricated viscous gravity currents, *Journal of Fluid*
637 *Mechanics.*, 766, 626-655, doi: 10.1017/jfm.2015.30, 2000.

638 Kyrke-Smith, T.M., Katz, R.F., and Fowler, A.C.: Subglacial hydrology and the formation of
639 ice streams, *Proceedings of the Royal Society.*, A 470(2161), 20130494, doi:
640 10.1098/rspa.2013.0494, 2014.
641

642 Le Brocq, A. M., Ross, N., Griggs, J.A., Bingham, R.G., Corr, H.F.J., Ferraccioli, F., Jenkins,
643 A., Jordan, T.A., Payne, A.J., Rippin, D.M., and Siegert, M.J.: Evidence from ice shelves for
644 channelized meltwater flow beneath the Antarctic Ice Sheet, *Nat. Geosci.*, 6, 945–948, doi:
645 10.1038/ngeo1977, 2013.
646

647 Lelandais, T., Mourgues, R., Ravier, É., Pochat, S., Strzeczynski, P., and Bourgeois, O.:
648 Experimental modeling of pressurized subglacial water flow: Implications for tunnel valley
649 formation, *J. of Geophy. Res. Earth Surface.*, 121(11), 2022-2041, doi: 10.1002/2016JF003957,
650 2016.
651

652 Lewis, A. R., Marchant, D. R., Kowalewski, D. E., Baldwin, S. L., and Webb, L. E.: The age
653 and origin of the Labyrinth, western Dry Valleys, Antarctica: Evidence for extensive middle
654 Miocene subglacial floods and freshwater discharge to the Southern Ocean, *Geology.*, 34,
655 513–516, doi: 10.1130/G22145.1, 2006.

656 Livingstone, S. J., and Clark, C. D.: Morphological properties of tunnel valleys of the southern
657 sector of the Laurentide Ice Sheet and implications for their formation, *Earth Surface*
658 *Dynamics*,4,567-589, doi: 10.5194/esurf-4-567-2016, 2016.

659
660 Livingstone, S. J., Utting, D. J., Ruffell, A., Clark, C. D., Pawley, S., Atkinson, N., and Fowler,
661 A. C.: Discovery of relict subglacial lakes and their geometry and mechanism of drainage. *Nat.*
662 *Commun.*, 7,11767, doi: 10.1038/ncomms11767, 2016.

663
664 Magnússon, E., Rott, H., Björnsson, H., and Pálsson, F., The impact of jökulhlaups on basal
665 sliding observed by SAR interferometry on Vatnajökull, Iceland, *J. Glaciol.*, 53, 232–240,
666 doi: 10.3189/172756507782202810, 2007.

667 Marciznek, S., and Piotrowski, J. A.: Groundwater flow under the margin of the last
668 Scandinavian ice Sheet Around the EckernföRde Bay, Northwest Germany, *Glacier Sci.*
669 *Environ. Chang.*, Knight, P.G., Blackwell Science Ltd 60–62, doi:
670 10.1002/9780470750636.ch10, 2006.

671 Margold, M., Stokes, C. R., Clark, C. D., and Kleman, J.: Ice streams in the Laurentide Ice
672 Sheet: a new mapping inventory, *J. Maps.*, 11, 380–395, doi: 10.1080/17445647.2014.912036,
673 2015.

674 Marshall, S. J.: Recent advances in understanding ice sheet dynamics, *Earth Planet. Sci. Lett.*,
675 240, 191–204, doi: 10.1016/j.epsl.2005.08.016, 2005.

676 Paola, C., Straub, K., Mohrig, D., and Reinhardt, L.: The unreasonable effectiveness of
677 stratigraphic and geomorphic experiments, *Earth-Science Rev.*, 97, 1–43, doi:
678 10.1080/17445647.2014.912036, 2009.

679 Paterson, W. S. B., Pergamon Kidlington, *The Physics of Glaciers*, Elsevier Science Ltd,
680 Great Britain, 480 pages, 1994.

681 Patterson, C. J.: Southern Laurentide ice lobes were created by ice streams: Des Moines Lobe
682 in Minnesota, USA, *Sediment. Geol.*, 111, 249–261, doi: 10.1016/S0037-0738(97)00018-3,
683 1997.

684 Payne, A. J., and Dongelmans, P. W.: Self-organization in the thermomechanical flow of ice
685 sheets. *J. Geophys. Res. Solid Earth.*, 102, 12219–12233,doi: 10.1029/97JB00513, 1997.

686
687 Perol, T., and Rice, J. R.: Shear heating and weakening of the margins of West Antarctic ice
688 streams, *Geophys. Res. Lett.*, 42, 3406–3413, doi: 10.1002/2015GL063638, 2015.

689

690 Peters, L. E., Anandakrishnan, S., Alley, R. B., and Smith, A. M., Extensive storage of basal
691 meltwater in the onset region of a major West Antarctic ice stream, *Geology.*, 35, 251–254,
692 doi: 10.1130/G23222A.1, 2007.

693 Ravier, E., Buoncristiani, J. F., Menzies, J., Guiraud, M., Clerc, S., and Portier, E.: Does
694 porewater or meltwater control tunnel valley genesis? Case studies from the Hirnantian of
695 Morocco, *Palaeogeogr. Palaeoclimatol. Palaeoecol.*, 418, 359–376, doi:
696 10.1016/j.palaeo.2014.12.003, 2015.

697 Raymond, C. F.: How do glaciers surge? A review, *J. Geophys. Res. Solid Earth.*, 92, 9121–
698 9134, doi: 10.1029/JB092iB09p09121, 1987.

699 Retzlaff, R., and Bentley, C. R.: Timing of stagnation of Ice Stream C, West Antarctica, from
700 short-pulse radar studies of buried surface crevasses, *J. Glaciol.*, 39, 553–561, doi:
701 10.3189/S0022143000016440, 1993.

702 Robel, A. A., Degiuli, E., Schoof, C., and Tziperman, E.: Dynamics of ice stream temporal
703 variability : Modes, scales, and hysteresis, *J. of Geophys. Res. Earth Surface.*, 118, 925–936,
704 doi: 10.1002/jgrf.20072, 2013.

705
706 Rothlisberger, H., and Lang, H., *Glacial hydrology. Glacio-Fluvial Sediment Transfer: An
707 Alpine Perspective*, Gurnell and Clark, John Wiley and Sons, New York New York. p 207-
708 284, 1987.

709 Shreve, R. L.: Movement of water in glaciers, *Journal of Glaciology.*, 11(62), 205-214, doi:
710 10.3189/S002214300002219X, 1972.

711 Siegfried, M. R., Fricker, H. A., Carter, S. P., and Tulaczyk, S.: Episodic ice velocity
712 fluctuations triggered by a subglacial flood in West Antarctica, *Geophys. Res. Lett.*, 43, 2640–
713 2648, doi: 10.1002/2016GL067758, 2016.

714
715 Stearns, L. A., Smith, B. E., and Hamilton, G. S.: Increased flow speed on a large East Antarctic
716 outlet glacier caused by subglacial floods, *Nat. Geosci.*, 1, 827–831, doi: 10.1038/ngeo356,
717 2008.

718
719 Vaughan, D. G., Corr, H. F. J., Smith, A. M., Pritchard, H. D., and Shepherd, A.: Flow-
720 switching and water piracy between Rutford Ice Stream and Carlson Inlet, West Antarctica.
721 *Journal of Glaciology.*, 54, 41–48, doi: 10.3189/002214308784409125, 2008.

722 Vaughan, D.G., J.C. Comiso, I. Allison, J. Carrasco, G. Kaser, R. Kwok, P. Mote, T. Murray,
723 F. Paul, J. Ren, E. Rignot, O. Solomina, K. Steffen and T. Zhang, 2013: Observations:
724 Cryosphere. In: *Climate Change 2013: The Physical Science Basis. Contribution of Working
725 Group I to the Fifth Assessment Report of the Intergovernmental Panel on Climate Change*
726 [Stocker, T.F., D. Qin, G.-K. Plattner, M. Tignor, S.K. Allen, J. Boschung, A. Nauels, Y. Xia,
727 V. Bex and P.M. Midgley (eds.)]. Cambridge University Press, Cambridge, United Kingdom
728 and New York, NY, USA
729

730 Winsborrow, M. C. M., Clark, C. D., and Stokes, C. R.: What controls the location of ice
731 streams?, *Earth-Science Rev.*, 103, 45–59, doi: 10.1016/j.earscirev.2010.07.003, 2010.